Cell Reports
Physical Science

CellPress
OPEN ACCESS

Article

Thermal-controlled cholesteric liquid crystal wavelength filter lens for photosensitive epilepsy treatment

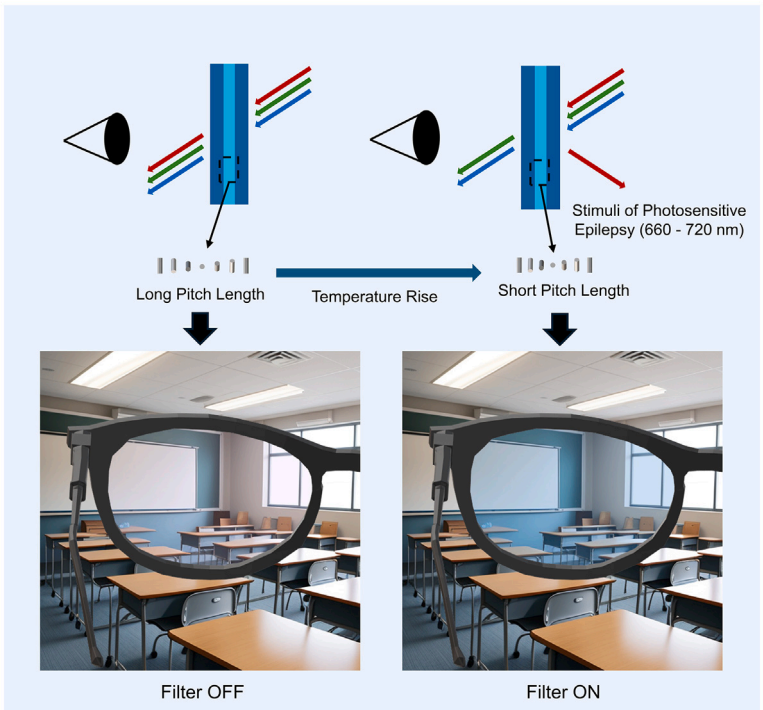

Xia et al. present a thermal-controlled cholesteric liquid crystal lens for photosensitive epilepsy patients by dynamically blocking harmful wavelengths. The lens can achieve over 98% light cutoff at critical wavelengths, and the filter can be switched via temperature variation.

Yuanjie Xia, Zubair Ahmed, Affar Karimullah, Nigel Mottram, Hadi Heidari, Rami Ghannam

yuanjie.xia@glasgow.ac.uk (Y.X.)
rami.ghannam@glasgow.ac.uk (R.G.)

Highlights

CLC materials are employed in reconfigurable color-filter lenses

These lenses can cut off specific wavelengths to mitigate photosensitive epilepsy

The reflection band of the CLC lenses is affected by temperature changes

An electronic control system is used to manipulate the reconfigurable lenses

Xia et al., Cell Reports Physical Science 5, 102158
September 18, 2024 © 2024 The Authors. Published by Elsevier Inc.
https://doi.org/10.1016/j.xcrp.2024.102158

Cell Reports
Physical Science

CellPress
OPEN ACCESS

Article

Thermal-controlled cholesteric liquid crystal wavelength filter lens for photosensitive epilepsy treatment

Yuanjie Xia,[1,*] Zubair Ahmed,[2] Affar Karimullah,[3] Nigel Mottram,[4] Hadi Heidari,[1] and Rami Ghannam[1,5,*]

SUMMARY

Cholesteric liquid crystals (CLCs) exhibit optical properties that are highly responsive to temperature or electric fields. Here, we report an approach to aiding in photosensitive epilepsy treatment by developing a thermal-controlled CLC wavelength filter lens. This lens demonstrates exceptional optical tunability, enabling it to dynamically change its stopband in response to temperature changes. At room temperature, the stopband of the CLC lens is outside the visible spectrum, rendering the lens functionally similar to normal glass. As the temperature rises to 36.5°C, the lens efficiently blocks light within the 660- to 720-nm wavelength range, which is the known trigger wavelength for photosensitive epilepsy. CLC materials with opposite handedness are used to achieve over 98% light cutoff at the stopband. We propose a control system for dynamically controlling the temperature in real time. The tunable lenses offer a solution for mitigating the effects of specific light stimuli on affected individuals.

INTRODUCTION

Liquid crystals (LCs) are a unique state of matter that combines the properties of both crystals and liquids. They exist in a phase between solid crystals and liquids, where their molecules exhibit some degree of order, similar to crystals, yet retain the fluidity of a liquid. This ordered arrangement gives LCs a property called anisotropy, meaning they exhibit different physical characteristics, such as electrical conductivity and refractive index, depending on the direction. Additionally, the spacing between LC molecules is similar to liquids, allowing them to flow freely. Furthermore, the behavior of LCs is sensitive to changes in both electric field and temperature, leading to alterations in their optical, electrical, and physical properties.[1,2] In fact, the variation of temperature can cause phase transitions between the smectic, nematic, and isotropic phases.[3]

A cholesteric LC (CLC) is a type of nematic (N)LC with helical molecular arrangement, as shown in Figure 1. A CLC cell can be divided into multiple sublayers, with the orientation of the directors varying between them. This variation is periodic, where the pitch length "P" represents the distance of the directors rotating 360° on a perpendicular axis. The pitch length is affected by various factors, including the temperature and composition of the CLC material.[4] The helical structure of a CLC material throughout the cell results in its special properties, including selective reflection, optical rotation, and circular dichroism.[5] Selective reflection means CLC materials can reflect certain wavelengths of light based on their physical properties, which is

[1]University of Glasgow, James Watt School of Engineering, Glasgow G12 8QQ, UK

[2]University of Birmingham, Neuroscience and Ophthalmology, Institute of Inflammation and Ageing, Birmingham B15 2TT, UK

[3]University of Glasgow, School of Chemistry, Glasgow G12 8QQ, UK

[4]University of Glasgow, School of Mathematics and Statistics, Glasgow G12 8QQ, UK

[5]Lead contact

*Correspondence:
yuanjie.xia@glasgow.ac.uk (Y.X.),
rami.ghannam@glasgow.ac.uk (R.G.)

https://doi.org/10.1016/j.xcrp.2024.102158

This is an open access article under the CC BY license (http://creativecommons.org/licenses/by/4.0/).

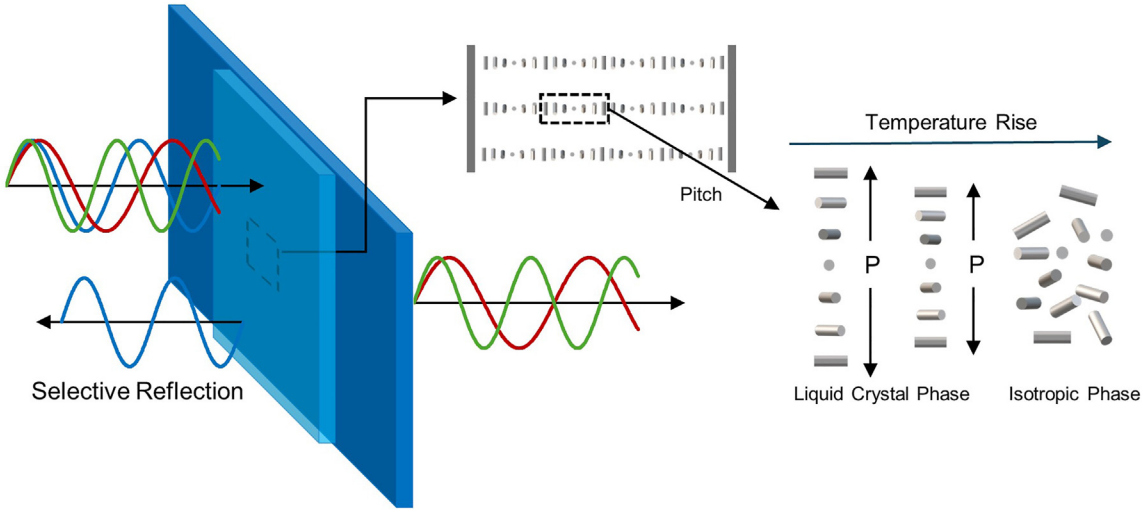

Figure 1. Schematic diagram of a thermal-controlled CLC lens that can reflect certain wavelengths of light

also known as Bragg reflection.[6] Specifically, when incident light interacts with the helical structure of CLC material, some light waves that align with the pitch of the helix exhibit constructive interference, which are reflected in a distinct direction. Noticeably, CLC materials of different handedness can selectively reflect different circularly polarized light in a certain wavelength range. For example, the chiral structure of left-handed CLC (LHCLC) material can selectively reflect left-handed circularly polarized light, with the reflect waveband determined by pitch length. Therefore, a CLC-based optic filter is designed on the basis of its properties to block certain wavelengths of light. For example, excessive exposure to blue light from electronic devices might induce photoreceptor damage and biorhythm disorder, which could be prevented by color-filtered glasses.[7,8] Moreover, the selective reflection can be utilized to prevent photo-triggered diseases—for example, dyslexia[9,10] and photosensitive epilepsy.[11,12]

Photosensitive epilepsy is a type of epilepsy that is triggered by exposure to flashing or flickering lights or certain visual patterns. Seizures can vary in severity and range from brief episodes of altered consciousness to convulsions and loss of consciousness.[13] The trigger for photosensitive epilepsy is visual stimuli that cause rapid and repetitive changes in the intensity or patterns of light. This can include flickering lights, flashing lights, or contrasting geometric patterns. Common sources of visual triggers include video games, television shows or movies, and strobe lights at concerts or parties. In particular, light with wavelengths of 660–720 nm can trigger photosensitive epilepsy.[14,15] Previous research suggests that color-filtered glasses have been used to treat epilepsy by blocking the light waveband that triggers epilepsy.[16] These colored glasses can filter around 50% of red light, which significantly reduces symptoms of epilepsy, including dizziness due to fluorescent lighting and aura caused by computer screens.

Conventional epilepsy treatment involves colored glasses that are fixed and cannot adjust their optical properties according to the environment. However, epilepsy patients are only likely to be exposed to light that triggers photosensitive epilepsy in a few scenarios, such as using a smartphone or playing video games. Therefore, the use of conventional colored glasses is inconvenient for patients. To address this issue, we have proposed a CLC-based tunable color filter for epilepsy treatment

that can switch its working mode to adapt to different environments. A CLC-based lens can be designed to block the band of light from 660 to 720 nm, and the wavelength of the block band can be controlled by temperature variation. Additionally, we have proposed a dual-layer CLC lens configuration in which LHCLC and right-handed CLC (RHCLC) layers are cascaded to provide maximum cutoff of the target wavelength from 660 to 720 nm.[17,18] In our design, the LHCLC and RHCLC are encapsulated by glass slides and optical adhesive. Three pieces of glass were used to create two LC cells for the two CLC materials with opposite handedness. This dual-layer CLC cell structure was first proposed by Mitov and Dessaud.[19]

In the literature, researchers have previously used CLCs to selectively reflect or transmit specific wavelengths of light based on temperature changes.[20,21] The temperature of the CLC filter can be controlled to change the pitch of the CLC material, causing a change in the reflected or transmitted wavelength. The pitch of the LC helix is temperature dependent, and previous research has used a transparent electrode to generate heat. When the pitch of the CLC matches the wavelength of the incident light, the light is reflected and creates a specific band of color. Previous researchers have found the relationship between applied voltage and LC cell temperature and then obtained the relationship between voltage and center frequency of the reflection band. However, the mapping from voltage to reflect waveband is not precise. The effect of environmental temperature on the LC cell cannot be ignored, which can result in systematic errors. For instance, lower room temperature will lead to higher heat dissipation, which in turn will cause lower LC cell temperature when the input power is the same. This systematic error can significantly affect the precision of the waveband filter in practical use. To address this issue, we proposed the incorporation of a built-in temperature sensor in the CLC cell to monitor the temperature of the CLC material in real time.

RESULTS

Theory and calculations

To design a waveband filter for photosensitive epilepsy treatment, the target wavelength is between 660 and 720 nm, which would trigger photosensitive epilepsy. E7 is a specific mixture of LC compounds with a nematic phase, which consists of a mixture of various LC compounds, including 5CB, 7CB, 8OCB, and 5CT. Compared with other pure substances of LC material, E7 demonstrates significant stability at a wide range of temperatures. It exhibits a nematic phase from approximately −55°C to 60°C, where, for example, 5CB is in LC phase only from 22.5°C to 35°C.[22–25] Therefore, E7 has been extensively used in LC display technologies. To prepare a CLC material to block the target waveband, a nematic LC material needs to be mixed with chiral dopants to introduce chirality, which will result in the helical structure of a nematic LC material. The ratio between the nematic LC host E7 and the chiral dopant will affect the pitch length P and other characteristics of the CLC. Here, left-handed chiral dopant (S)-2-octyl 4-[4-(hexyloxy)benzoyloxy] benzoate (S811) and right-handed chiral dopant(R)-2-octyl 4-[4-(hexyloxy) benzoyloxy]benzoate (R811) were employed in our design, as shown in Figure 2. These two chiral dopants have the same molecular formula, but they are able to introduce opposite chirality to NLC materials due to their opposite chemical structure.

The central wavelength and bandwidth of Bragg reflection can be calculated using refractive indexes and pitch length. Noticeably, due to the anisotropy of LC material, the refractive index has different values along and perpendicular to the LC director,

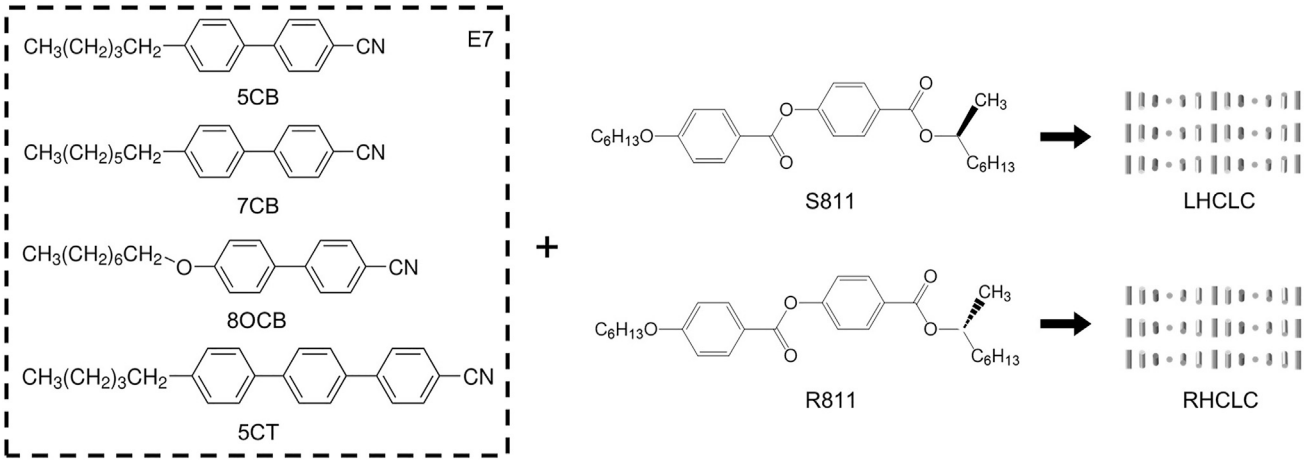

Figure 2. The chemical structure of related LC materials and chiral dopants

Opposite-handedness of chiral dopants can introduce different orientations of the helical structure.

which are n_e and n_o, respectively.[26] The central wavelength and bandwidth of Bragg reflection at normal incidence could be calculated by[27]

$$\lambda_{central} = nP \quad \text{(Equation 1)}$$

$$\Delta\lambda = \Delta nP, \quad \text{(Equation 2)}$$

where n is the average refractive index and could be calculated by[28]

$$n^2 = \frac{\left(n_e^2+2n_o^2\right)}{3}. \quad \text{(Equation 3)}$$

The refractive index of E7 n_o and n_e is 1.53 and 1.75, respectively.[25,29] According to the formula, the target pitch length is 429 nm and the width of the notch band is 96.8 nm, which can cover the wavelength of the CLC cell. Subsequently, the transmittance of the CLC cell at different wavelengths could be simulated using the Berreman 4×4 method.[30,31] Based on articles from Berreman and Schubert, the Berreman 4×4 matrix method was developed to solve the propagation of plane waves in anisotropic layers.[32] In the Berreman 4×4 method, the CLC layer is divided into multiple layers, which consider factors like reflection, transmission, and phase changes that occur at each interface between different layers. The propagation of the light wave in the CLC sample could be represented by Maxwell's equations[4,33]:

$$\nabla \cdot \mathbf{D} = 0 \quad \text{(Equation 4)}$$

$$\nabla \cdot \mathbf{B} = 0 \quad \text{(Equation 5)}$$

$$\nabla \times \mathbf{E} = -\frac{\partial \mathbf{B}}{\partial t} = ik_0\mathbf{H} \quad \text{(Equation 6)}$$

$$\nabla \times \mathbf{H} = \frac{\partial \mathbf{D}}{\partial t} = -ik_0\epsilon\mathbf{E}. \quad \text{(Equation 7)}$$

Assuming light wave propagation is along the z axis, Maxwell's equations result in a propagation equation with the transverse components (Ex, Ey, Hx, Hy). After that, the propagation of the electromagnetic wave in the isotropic media could be calculated via the equation

$$\frac{\partial \phi}{\partial t} = -ik_0\mathcal{D}\phi(z), \quad \text{(Equation 8)}$$

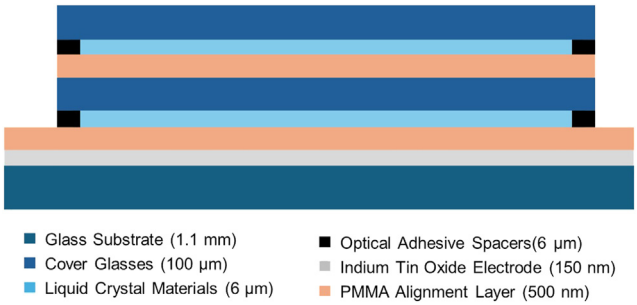

Figure 3. Cross-sectional view of the CLC lens

Notably, the schematic diagram illustrates the device architecture.The figure is not drawn to scale, with certain layers exaggerated in thickness for clarity and visibility.

where $\mathcal{D}$ is Berreman's 4×4 matrix:

$$\mathcal{D} = \begin{bmatrix} -\eta\frac{\varepsilon_{31}}{\varepsilon_{33}} & 1-\frac{\eta^2}{\varepsilon_{33}} & -\eta\frac{\varepsilon_{32}}{\varepsilon_{33}} & 0 \\ \varepsilon_{11}-\frac{\varepsilon_{13}\varepsilon_{31}}{\varepsilon_{33}} & -\eta\frac{\varepsilon_{13}}{\varepsilon_{33}} & \varepsilon_{12}-\frac{\varepsilon_{13}\varepsilon_{32}}{\varepsilon_{33}} & 0 \\ 0 & 0 & 0 & 1 \\ \varepsilon_{21}-\frac{\varepsilon_{23}\varepsilon_{31}}{\varepsilon_{33}} & -\eta\frac{\varepsilon_{23}}{\varepsilon_{33}} & \varepsilon_{22}-\frac{\varepsilon_{23}\varepsilon_{32}}{\varepsilon_{33}}-\eta^2 & 0 \end{bmatrix}, \quad \text{(Equation 9)}$$

The components of the incident light $\eta = k_x/k_0$ are constant throughout the sample. Subsequently, the output light wave of a single layer could be calculated by integrating Equation 8 along the z axis, as shown below:

$$\varphi(z+\delta z) = e^{-ik_0\mathcal{D}(z)\delta z}\varphi(z). \quad \text{(Equation 10)}$$

Therefore, since the CLC layer is divided into multiple thin films, the overall transmittance of light waves can be calculated by

$$\varphi_t = \prod_{i=1}^{N}\varphi(\delta z_i). \quad \text{(Equation 11)}$$

To prevent photosensitive epilepsy, 660- to 720-nm wavelengths of light need to be filtered by the glasses. Therefore, the transmittance of a CLC cell with a central wavelength of 690 nm is simulated, and the result is demonstrated in the following section.

System design

The CLC lens consists of indium tin oxide (ITO)-coated glass, an alignment layer, spacers, the CLC layers, and cover glasses, where the CLC layer includes LHCLC and RHCLC material. Each of the layers is encapsulated by two pieces of glass and UV adhesive glue. The schematic diagram of a dual-layer CLC lens is demonstrated in Figure 3. It is noticeable that the figure is not drawn to scale. In addition, the thickness of each layer is illustrated in the figure. The detailed process of fabricating a dual-layer CLC lens is discussed in the experimental procedures.

To tune the CLC lens, a system was designed to monitor and dynamically control the selective reflection band of the CLC lens in real time, as shown in Figure 4A. As previously discussed, the selective reflection band is related to the pitch length of CLC material, and the pitch length can be modulated by adjusting the temperature; thus, here, we proposed a feedback system for real-time temperature control. Specifically, a direct current voltage source was employed on the ITO-coated glass to

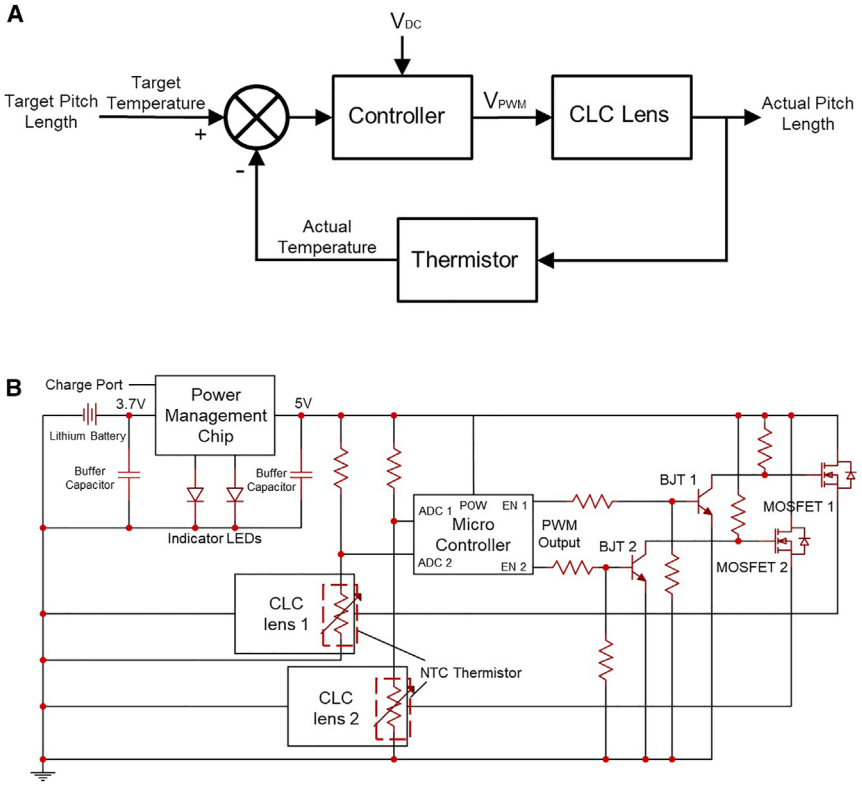

Figure 4. Proposed system and circuit design

(A) The feedback system for dynamically controlling the pitch length of CLC lenses.

(B) Simplified schematic diagram of the controller system design.

generate heat. A negative temperature coefficient (NTC) thermistor was placed on a thin cover glass to continuously monitor the variation in temperature. Notably, NTC means that the resistance of the thermistor decreases as its temperature increases. The thickness of the cover glass is around 100 μm, which could significantly minimize the impact of heat dissipation within the glass layers and enable quicker responses to temperature shifts. After that, the difference between the actual temperature and the target temperature is used as input to an external controller, which can adjust the voltage added to the CLC cell. Subsequently, the controller produces a pulse width modulation (PWM) signal to control a metal oxide semiconductor field-effect transistor (MOSFET), which varies the voltage across the ITO glass via different duty cycles, as shown in Figure 4A. The MOSFET acts as a relay, preventing potential large currents on the ITO glass from affecting the operation of the microcontroller. Moreover, a proportional-integral-derivative (PID) algorithm was employed within the system to dynamically control the temperature, which can enable the system to quickly stabilize at the target temperature.

Subsequently, the electronic system was designed according to the requirements, which resulted in a simplified schematic diagram of the system shown in Figure 4B. The system is powered by a 3.7-V lithium battery, which is ideal for wearable devices. A power management module is used to boost the 3.7-V input to 5 V. To convert the variations of thermistor resistance into voltage variations, a voltage division circuit was used. The microcontroller reads the voltage variations through its analog-to-digital converter (ADC) pin. Additionally, the microcontroller can communicate with external devices through Bluetooth, enabling users to switch the modes of

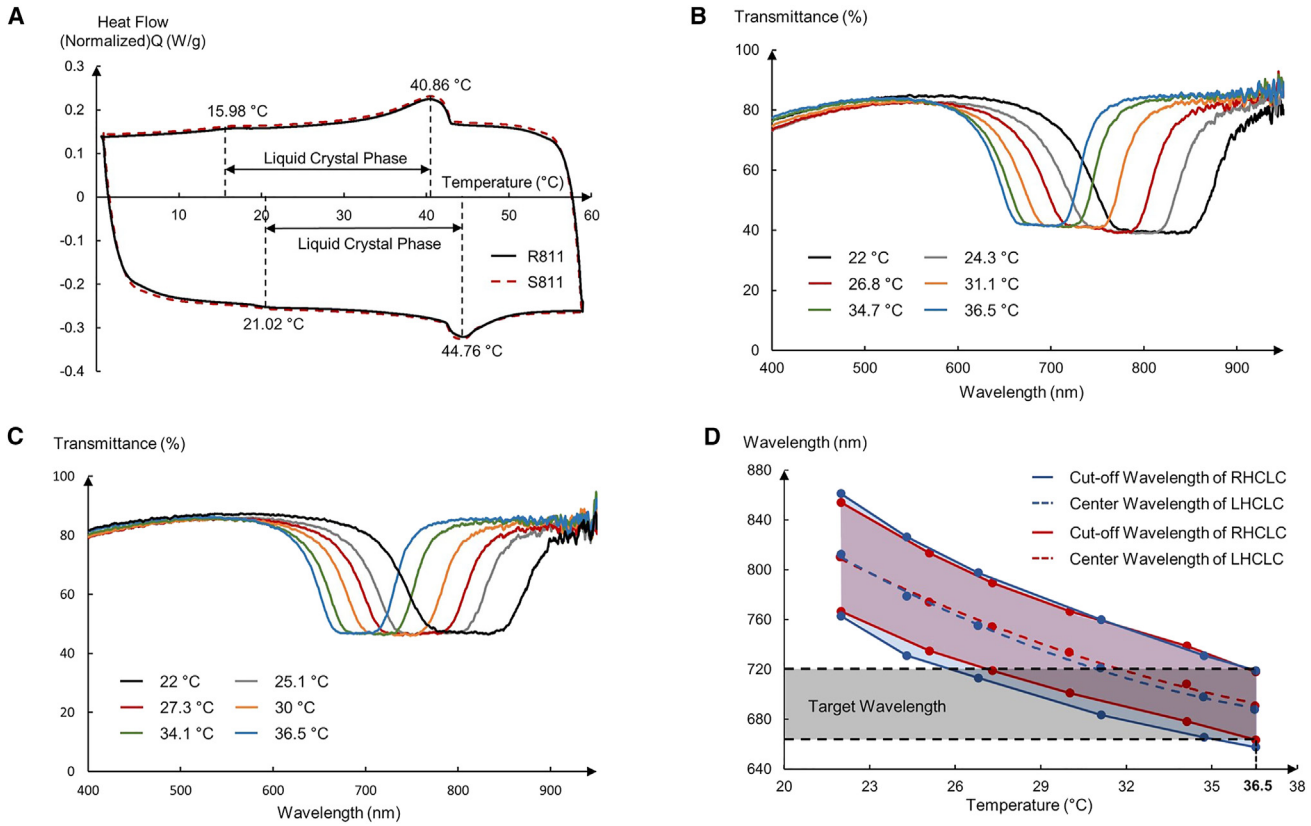

Figure 5. Experimental data of CLC materials

(A) DSC analysis of 21 wt % S811:E7 LHCLC and R811:E7 RHCLC material.

(B) The selective reflection of LHCLC at different temperatures.

(C) The selective reflection of RHCLC at different temperatures.

(D) The cutoff wavelength and center wavelength of selective reflection at different temperatures.

the glasses through a smartphone or computer. After the microcontroller receives the temperature data from the thermistor, it uses a PID algorithm to convert the difference between the target temperature and actual temperature into a control signal. The control signals were PWM waves, which enabled the duty cycle to be adjusted to regulate the voltage applied across the CLC lenses. Bipolar junction transistors were used as a current source in the system and coupled with resistors to produce enabling signals for MOSFETs. Finally, the adjusted voltage was applied to the CLC lenses to maintain a selective reflection band at the target wavelength.

Prototype testing and evaluation

To block light within the wavelength range of 660–720 nm, 21 wt % LHCLC and RHCLC materials were employed. Subsequently, DSC analysis was executed to measure the heat flow of the materials, so that the phase transition temperature could be measured. According to the result, two materials exhibit similar thermal properties, as shown in Figure 5A. During the heating process, the 21 wt % CLC materials exhibited in the LC phase from 21.02°C to 44.76°C. Additionally, this material exhibited in the LC phase from 15.98°C to 40.86°C during the cooling cycle. Therefore, the melting point and clear point of the CLC material are from 15.98°C to 21.02°C and from 40.86°C to 44.76°C, respectively. Significantly, the temperature range that the material exhibits in LC phase is narrower compared to the LC material E7, as mentioned above, which is caused by the mixture of chiral dopant material. To

ensure the materials are in the LC phase, the temperature of the CLC cell needs to be controlled within 21.02°C–40.86°C. However, when the temperature is close to the clear point, the heat will destroy the helical structure of the CLC material, resulting in the opacity of the CLC cell. To prevent this, the operation temperature is kept lower than 38°C to ensure the transmittance. In addition, the transmittance of LHCLC and RHCLC cells at different temperatures was measured, as shown in Figures 5B and 5C. It is noticeable that the waveform of the transmittance of LHCLC filters was similar to that of RHCLC filters but not exactly the same. For example, the selective reflection band of LHCLC material is slightly wider than that of RHCLC material. Moreover, LHCLC demonstrates lower transmittance at the center wavelength of the selective reflection band. This difference is due to the difference in purity of the chiral dopants S811 (95%) and R811 (98%). According to the measurement, the relationship between wavelength and temperature can be obtained, as demonstrated in Figure 5D. The trigger wavelength of photosensitive epilepsy is from 660 to 720 nm, which can be blocked by these two CLC materials at 36.5°C.

Therefore, 36.5°C was set as the target temperature range to activate the optical filter of CLC lenses to protect epilepsy patients. The visible spectrum varies among individuals, but it is commonly considered to span from 400 to 720 nm.[34,35] At room temperature (approximately 25°C), the reflection band of the CLC lens is not in the visible light range; thus, the filter can be regarded as "off." At 36.5°C, the reflection band is located at around 660–720 nm, where the filter can be regarded as "on." Therefore, based on its optical properties, a tunable CLC filter was designed as a lens that could be switched via temperature. As shown in Figure 6, the selective reflections of CLC materials with 429- and 503-nm pitch length were simulated using the Berreman 4×4 method, which could be matched with the experimental result of 21 wt % LHCLC and RHCLC materials at 22°C and 36.5°C.

A prototype of the color filter glasses is demonstrated in Figure 7A. The figure showcases the alteration in background color when the filter was switched on and off. Moreover, the infrared thermal profile images of the CLC lens showcase that heat is uniformly distributed, which ensures the uniformity of the reflection of the target wavelength. The printed circuit board (PCB) design for the control system is demonstrated on the right side of the figure. The PCB is 48×20 mm^2 in size, which is suitable for wearable applications. Subsequently, the spectrum diagrams of dual-layer CLC lenses are shown in Figure 7B. When the filter is off, the CLC lenses allow maximum transmittance in the visible spectrum. As the temperature rises to 36.5°C, the filter is switched on, which is able to block over 98% of the target wavelength of light. The heating cycle is shown in Figure 7C. Here, we repeat the heating cycle five times, including heating and dynamic temperature control and cooling process, which showed good stability of the system.

DISCUSSION

This paper presents a novel tunable glasses lens for photosensitive epilepsy treatment using CLC materials. In the Results section, the lenses exhibited outstanding optical tunability and were able to vary the reflection band through temperature. At room temperature (around 25°C), the reflection band of the CLC lens exceeded 720 nm, which is beyond the visible spectrum. Therefore, the lenses exhibited good transmittance within the visible spectrum, making them appear like normal glasses lenses. To protect epilepsy patients, the lenses are required to be heated to 36.5°C, ensuring that light with a wavelength between 660 and 720 nm is blocked. In evaluating the design, we noticed that the prototype worked functionally when

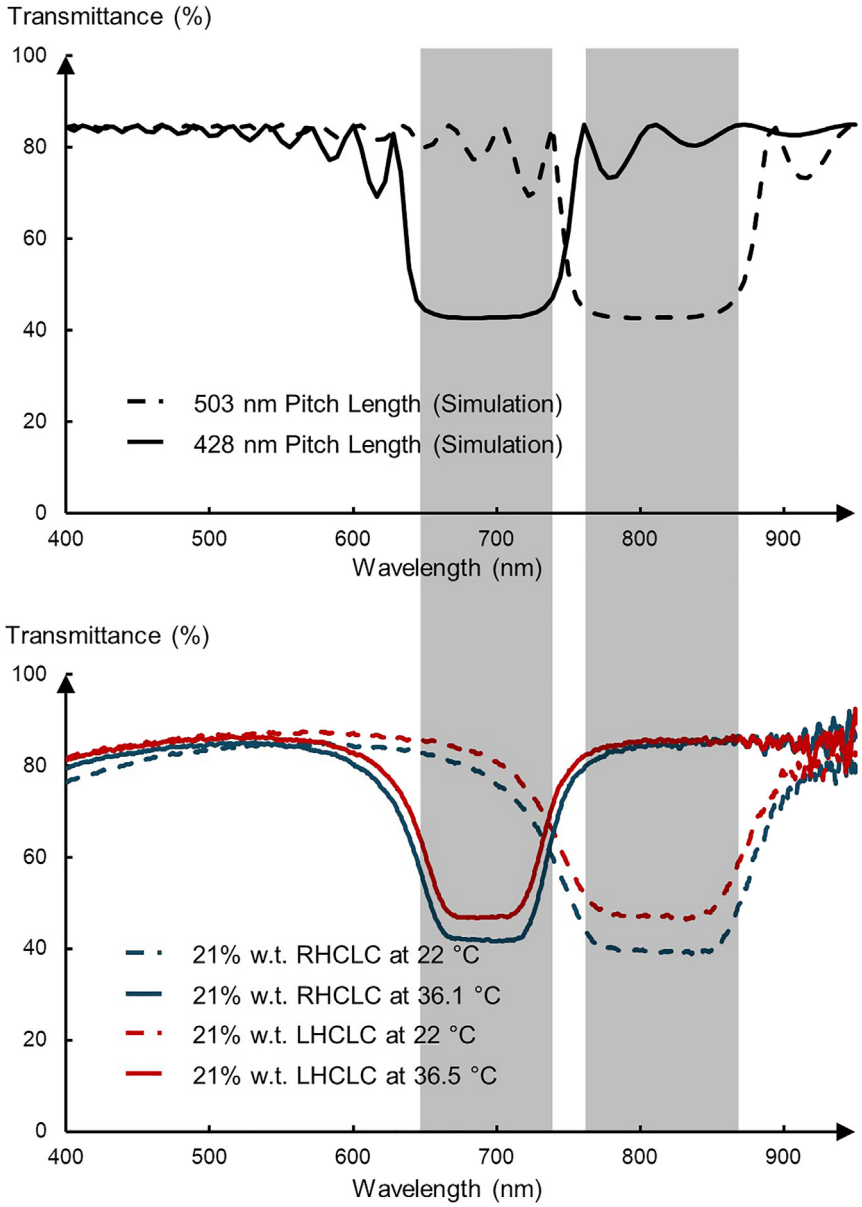

Figure 6. Comparison of simulation and experimental results of transmittance at different wavelengths

The simulation results of the CLC cell with pitch lengths of 429 and 503 nm are compared to experimental results of 21 wt % RHCLC and LHCLC at 22°C and 36.5°C.

room temperature did not exceed 26°C. It makes the tunable lenses suitable for the majority of scenarios since the trigger light sources usually come from digital devices—for example, video games and movies. If the environmental temperature exceeds 26°C, a portion of the reflection band falls within the visible spectrum, which might influence the user experience. To cater to usage demand at high temperatures, chiral dopants with high helical twisting power could be introduced to modify the sensitivity of CLC materials to temperature. Additionally, it is a general conclusion that light within 660 and 720 nm can trigger photosensitive epilepsy. However, different individuals have different trigger wavelengths.[36,37] This issue could be solved by calibrating the working temperature of the CLC lenses. Moreover, the

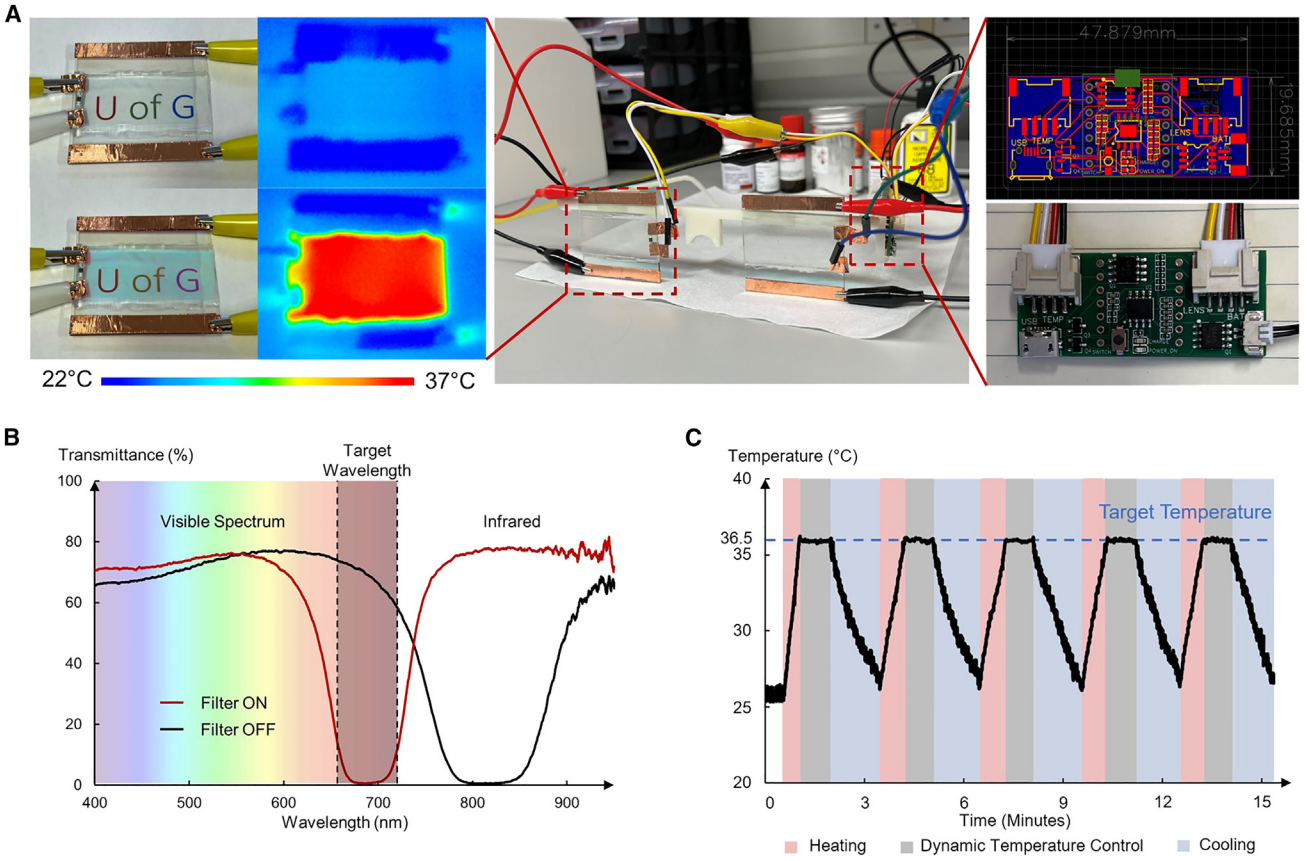

Figure 7. Prototype of the tunable CLC eyeglass and its performance

(A) The prototype of tunable glasses for photosensitive epilepsy.

(B) The transition of the stopband when switching the filter on and off.

(C) Heating cycle of the CLC lens.

weight percentage of CLC materials could be further adjusted to cater to the requirements of users.

Furthermore, this tunable eyeglass can be extended to other applications. For example, dyslexia is known as a reading disorder that can also affect writing and spelling ability. Moreover, up to 20% of the general population may be affected by different degrees of dyslexia.[38] Based on the literature regarding dyslexia, researchers discovered that wearing yellow or blue filter glasses can help dyslexia patients.[39,40] Apart from that, reading efficiency can be improved by highlighting words or sentences.[41] Therefore, tunable color filter glasses can offer assistance to dyslexia patients to focus on reading. Additionally, researchers discovered that excessive exposure to blue light, particularly emitted from digital screens and light-emitting diode lighting, can disrupt circadian rhythms by suppressing melatonin production, leading to sleep disturbances and potential long-term implications for overall well-being.[42–44] Tunable blue light filter glasses could be then developed to mitigate prolonged exposure to blue light for computer users.[45,46] The tunable feature would enable the users to switch the glasses to normal mode in daily life.

Limitations of the study

The main challenge with our current prototype design is reducing the heating and cooling time. To address this issue, refining the lens structure or incorporating

advanced electrodes with enhanced thermal conductivity could accelerate temperature changes. On the materials side, exploring CLC materials with higher temperature sensitivity might provide a solution, as they can achieve larger stopband shifts with smaller temperature changes.

Additionally, the application of CLC glasses has been limited to indoor environments where the room temperature must remain below 26°C for the filter to switch off. This problem could be solved by using new CLC materials with an operating temperature closer to 40°C. This temperature is slightly above room temperature but still comfortable for users.[47]

Moreover, variations in the incidence angle can affect the reflection band. Our current design assumes that users will face the light source directly, which commonly happens when watching a movie or playing a video game. To allow the lens to block the target light band from different angles, one possible solution is to introduce curvature to the lens substrate.

It is also important to note that while our study demonstrates advancements in the tunability of color filter glasses, further clinical trials are necessary to establish the efficiency of this technology for managing photosensitive epilepsy. Our current work focuses on improving the adaptability of glasses in various environments and does not directly assess their clinical effectiveness in treating the condition.

Despite the presence of defects, this prototype successfully demonstrated the feasibility of employing CLC lenses to filter certain wavelengths of light that are harmful to people. The lens exhibited tunability through temperature variation, showcasing its potential as an adaptable and responsive solution for filtering harmful light. Further refinement and optimization of CLC lenses could lead to a more robust and reliable solution for practical applications.

EXPERIMENTAL PROCEDURES

Resource availability

Lead contact

Further information and requests for resources should be directed to and will be fulfilled by the lead contact, Rami Ghannam (rami.ghannam@glasgow.ac.uk).

Materials availability

All materials generated in this study are available from the lead contact without restriction.

Data and code availability

All data are available in the main text. Other relevant data are available from the corresponding authors on reasonable request. We have uploaded the relevant codes to Zenodo. They can be downloaded from https://doi.org/10.5281/zenodo.12794967.

Preparation of CLC

Researchers have previously studied how different proportions of NLC E7 and chiral dopant S811 would result in different pitch lengths.[20] Therefore, 21 wt % CLC materials were employed in this work to block trigger wavelength for photosensitive epilepsy from 660 to 720 nm. According to our simulation, CLC materials with a 429-nm pitch length are required to block light in the range. Additionally, cascading an LHCLC cell and an RHCLC cell can block over 95% of light within the target band. To prepare LHCLC material with a 429-nm pitch length, E7 (SYNTHON Chemicals)

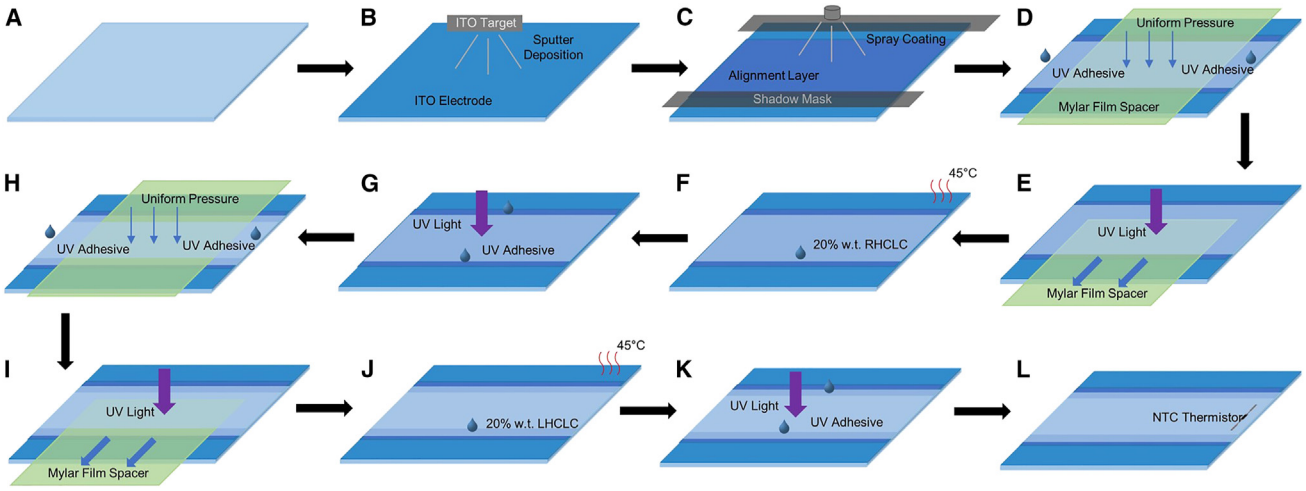

Figure 8. Fabrication process of a dual-layer CLC

(A) Obtain a 5 × 5-cm^2 glass substrate.
(B) Sputter coat the ITO electrode.
(C) Spray coat the alignment layer with shadow mask.
(D) Fix two glass slides with Mylar film spacer and UV adhesive.
(E) Cure UV adhesive and extract film spacer.
(F) Place a droplet of CLC material at the edge of the empty cell, and heat the sample to 45°C.
(G) After CLC material fills the gap between two glass slides, seal the two edges of the CLC cell with UV adhesive.
(H) Add another glass slide on top of the cell, and fix the gap with film spacer.
(I–K) Repeat steps (E)–(G).
(L) Mount a thermistor and PCB on the CLC cell for temperature monitoring.

and S811 (95%, Sigma-Aldrich) are mixed with 21 wt % at 50°C. Similarly, E7 and R811 (98%, Sigma-Aldrich) are mixed with 21 wt % at 50°C to prepare RHCLC material. The CLC materials were well mixed by ultrasonic bath for 30 min and cooled down to room temperature. Then, they became a thick and clouded fluid.

Sensor integration

To monitor the temperature in real time, a temperature-sensing system should be integrated into the lens. There are many optional sensors for temperature monitoring, including thermistors, thermocouples, and infrared thermometers. After evaluating the dimensions and characteristics of different sensors, the thermistor has been selected as a temperature sensor in the system. An NTC surface-mounted thermistor was integrated into the glass lens. Unlike PCBs, soldering electronic components on glass-based samples is challenging. First, the circuit was printed on cover glass using silver paint with a shadow mask. Second, the thermistor was adhered to the desirable position by optical adhesive NOA68 and exposed to UV light for 10 min. This step fixes the thermistor on the cover glass. After that, silver paint was used to establish a connection between the thermistor and wires.

Fabrication of LC cell

The fabrication of a CLC-based lens is demonstrated in Figure 8. In step A, the 50 × 50-mm glass substrate was cleaned with isopropyl alcohol in an ultrasonic bath for 5 min. This step cleans the substrate to ensure better adhesion of the electrode material to its surface. After that, as shown in step B, a 1,500-Å thick ITO layer was deposited on the glass substrate using a Moorfield sputter coater. The sheet resistance of this layer is around 13 Ω/sq, and its average transmittance in the visible spectrum is around 87%.

Step C involves coating the substrate with a layer of polymethyl methacrylate (4% solid content anisole solvent; AllResist) as an alignment layer. This is an effective topographical method for LC alignment.[48,49] Mechanical rubbing of the substrate surfaces in one direction using cloth creates microscopic grooves that guide the LC molecules to align parallel to the rubbing direction. The top glass slide was then placed on the bottom substrate with a 6-μm Mylar film spacer between them. Then, UV adhesive (NOA68) was applied to the cell's edge to fix the gap between the two substrates. Next, the cell was exposed to UV light to cure the adhesive material, and then the Mylar film spacer was removed. At this point, an empty LC cell was fabricated.

Subsequently, the cell was placed on a hot plate and heated to 45°C, and a droplet of 21 wt % CLC material was placed at one edge of the cell, where the LC material flowed into the empty cell due to surface tension. The temperature of the hot plate should be higher than the clear point of the LC material, allowing the LC material to transform into an isotropic phase and speed up the process. The next step was to seal the remaining two edges after the LC cell was filled with LC material to prevent leakage and contamination. All the previous steps, demonstrated in Figures 8A–8G, were for fabricating a single-layer LC cell. Subsequently, steps H–K involved repeating processes from D to G to fabricate another CLC layer. Finally, step I involved mounting an NTC thermistor onto the CLC cell to monitor its temperature in real time.

Measurement and characterization

The thicknesses of the electrode and alignment layers were measured via a profilometer (DektakXT, Bruker). The sheet resistance of the ITO electrode was measured using the four-point probe method with a Hall Effect Measurement System (Nanometrics). Thermal analysis was done using by differential scanning calorimeter instrument (Discovery DSC 25, TA Instruments). Here, the heating cycle was set from 0°C to 60°C (ramp 10°C/min) to measure the melting point and clear point of 21 wt % CLC materials. The heating cycle was repeated three times in the measurement. Noticeably, the observed differences in phase transitional points between heating and cooling processes arise from the enantiotropic and monotropic nature of LC materials, where phase transitional points during cooling have relatively smaller values compared with heating. The transmission spectrum of CLC lenses was measured by a spectrometer (USB2000+ fiber optic, Ocean Optics). During the measurement, the samples were heated to the target temperature, where the stopband was located at the trigger frequency of photosensitive epilepsy. Subsequently, the samples were cooled to room temperature, and six measurements of transmission spectrum were taken during the period, which enabled us to obtain the relationship between temperature and selective reflection band. An infrared thermal camera (Testo 865) was used to calibrate the thermistor after the fabrication of CLC cells. This step is to establish the correlation between temperature and the resistance of the thermistor. Noticeably, the calibration process is necessary for each individual CLC cell since discrepancies in thermistor resistance might cause system errors. Additionally, the infrared thermal camera was used to capture a thermal image of the sample to showcase that the sample was heated uniformly.

ACKNOWLEDGMENTS

This research was partially supported by the UK's Engineering and Physical Sciences Research Council (project number 323668, project name "ARTIFY").

AUTHOR CONTRIBUTIONS

Y.X. designed and carried out the experiments, analyzed the data, and wrote the manuscript. N.M. provided mathematics instruction for simulations. A.K., H.H., and R.G. helped design the experiments and provided equipment and materials for the experiments. Z.A. and R.G. conceived the idea for the study and edited the manuscript. All authors have approved the final manuscript.

DECLARATION OF INTERESTS

The authors declare no competing interests.

Received: March 1, 2024
Revised: May 8, 2024
Accepted: July 26, 2024
Published: August 20, 2024

REFERENCES

1. Ghannam, R., Xia, Y., Shen, D., Fernandez, F.A., Heidari, H., and Roy, V.A.L. (2021). Reconfigurable surfaces using fringing electric fields from nanostructured electrodes in nematic liquid crystals. Adv. Theory Simul. *4*, 2100058.

2. James, R., Willman, E., Ghannam, R., Beeckman, J., and Fernández, F.A. (2021). Hydrodynamics of fringing-field induced defects in nematic liquid crystals. J. Appl. Phys. *130*, 134701. https://doi.org/10.1063/5.0062532.

3. Vertogen, G., and De Jeu, W.H. (2012). Thermotropic Liquid Crystals, Fundamentals*vol 45* (Springer Science & Business Media).

4. Goodby, J.W., Collings, P.J., Kato, T., Tschierske, C., Gleeson, H., Raynes, P., and Vill, V. (2014). Handbook of Liquid Crystals*vol 8* (John Wiley & Sons).

5. Saeva, F.D., and Wysocki, J.J. (1971). Induced circular dichroism in cholesteric liquid crystals. J. Am. Chem. Soc. *93*, 5928–5929.

6. St John, W.D., Fritz, W.J., Lu, Z.J., and Yang, D.-K. (1995). Bragg reflection from cholesteric liquid crystals. Phys. Rev. E *51*, 1191–1198.

7. Tosini, G., Ferguson, I., and Tsubota, K. (2016). Effects of blue light on the circadian system and eye physiology. Mol. Vis. *22*, 61–72.

8. Bedrosian, T.A., and Nelson, R.J. (2017). Timing of light exposure affects mood and brain circuits. Transl. Psychiatry *7*, e1017.

9. Quercia, P., Feiss, L., and Michel, C. (2013). Developmental Dyslexia and Vision (Clinical Ophthalmology), pp. 869–881.

10. Pammer, K., and Lovegrove, W. (2001). The influence of color on transient system activity: Implications for dyslexia research. Percept. Psychophys. *63*, 490–500.

11. Parra, J., Kalitzin, S.N., Iriarte, J., Blanes, W., Velis, D.N., and Lopes da Silva, F.H. (2003). Gamma-band phase clustering and photosensitivity: is there an underlying mechanism common to photosensitive epilepsy and visual perception? Brain *126*, 1164–1172.

12. Porciatti, V., Bonanni, P., Fiorentini, A., and Guerrini, R. (2000). Lack of cortical contrast gain control in human photosensitive epilepsy. Nat. Neurosci. *3*, 259–263.

13. Harding, G.F., and Jeavons, P.M. (1994). Photosensitive Epilepsy*133* (Cambridge University Press).

14. Fisher, R.S., Harding, G., Erba, G., Barkley, G.L., and Wilkins, A.; Epilepsy Foundation of America Working Group (2005). Photic-and pattern-induced seizures: a review for the epilepsy foundation of america working group. Epilepsia *46*, 1426–1441.

15. Okudan, Z.V., and Özkara, Ç. (2018). Reflex epilepsy: triggers and management strategies. Neuropsychiatr. Dis. Treat. *14*, 327–337.

16. Wilkins, A.J., Baker, A., Amin, D., Smith, S., Bradford, J., Zaiwalla, Z., Besag, F.M., Binnie, C.D., and Fish, D. (1999). Treatment of photosensitive epilepsy using coloured glasses. Seizure *8*, 444–449.

17. Lee, K.M., Tondiglia, V.P., McConney, M.E., Natarajan, L.V., Bunning, T.J., and White, T.J. (2014). Color-tunable mirrors based on electrically regulated bandwidth broadening in polymer-stabilized cholesteric liquid crystals. Acs Photonics *1*, 1033–1041.

18. Jeong, M.-Y., and Kwak, K. (2019). Continuously tunable optical notch filter with functions of a mirror and a beam splitter. IEEE Photonics J. *11*, 1–10.

19. Mitov, M., and Dessaud, N. (2006). Going beyond the reflectance limit of cholesteric liquid crystals. Nat. Mater. *5*, 361–364.

20. Tzeng, S.-Y., Chen, C.-N., and Tzeng, Y. (2010). Thermal tuning band gap in cholesteric liquid crystals. Liq. Cryst. *37*, 1221–1224.

21. Froyen, A.A., Wübbenhorst, M., Liu, D., and Schenning, A.P. (2021). Electrothermal color tuning of cholesteric liquid crystals using interdigitated electrode patterns. Advanced Electronic Materials *7*, 2000958.

22. Bedjaoui-Alachaher, L., Bensaid, H., Gordin, C., and Maschke, U. (2011). Solubility effects of multicomponent liquid crystal blends towards poly (n-butyl-acrylate). Liq. Cryst. *38*, 1315–1320.

23. Elouali, M., Beyens, C., Elouali, F.Z., Yaroshchuk, O., Abbar, B., and Maschke, U. (2011). Dispersions of diamond nanoparticles in nematic liquid crystal/polymer materials. Mol. Cryst. Liq. Cryst. *545*, 77–1301.

24. Zannoni, C. (2022). Liquid Crystals and Their Computer Simulations (Cambridge University Press).

25. Xia, Y., Yuan, M., Dobrea, A., Li, C., Heidari, H., Mottram, N., and Ghannam, R. (2023). Reconfigurable wearable antenna for 5G applications using nematic liquid crystals. Nano Select *4*, 513–524. https://doi.org/10.1002/nano.202200209.

26. Dierking, I. (2003). Textures of Liquid Crystals (John Wiley & Sons).

27. Mitov, M. (2012). Cholesteric liquid crystals with a broad light reflection band. Adv. Mater. *24*, 6260–6276.

28. Jirón, V., and Castellón, E. (2022). The experimental average refractive index of liquid crystals and its prediction from the anisotropic indices. Phys. Chem. Chem. Phys. *24*, 7788–7796.

29. Meng, S., Kyu, T., Natarajan, L.V., Tondiglia, V.P., Sutherland, R.L., and Bunning, T.J. (2005). Holographic photopolymerization-induced phase separation in reference to the phase diagram of a mixture of photocurable monomer and nematic liquid crystal. Macromolecules *38*, 4844–4854.

30. Berreman, D.W. (1972). Optics in stratified and anisotropic media: 4× 4-matrix formulation. Josa *62*, 502–510.

31. Berreman, D.W. (1973). Optics in smoothly varying anisotropic planar structures: application to liquid-crystal twist cells. JOSA *63*, 1374–1380.

32. Schubert, M. (1996). Polarization-dependent optical parameters of arbitrarily anisotropic

homogeneous layered systems. Phys. Rev. B *53*, 4265–4274.

33. Yang, D.-K., and Wu, S.-T. (2014). Fundamentals of Liquid Crystal Devices (John Wiley & Sons).

34. Palczewska, G., Vinberg, F., Stremplewski, P., Bircher, M.P., Salom, D., Komar, K., Zhang, J., Cascella, M., Wojtkowski, M., Kefalov, V.J., and Palczewski, K. (2014). Human infrared vision is triggered by two-photon chromophore isomerization. Proc. Natl. Acad. Sci. USA *111*, E5445–E5454.

35. Schnapf, J.L., Kraft, T.W., and Baylor, D.A. (1987). Spectral sensitivity of human cone photoreceptors. Nature *325*, 439–441.

36. Takahashi, Y., Fujiwara, T., Yagi, K., and Seino, M. (1999a). Photosensitive epilepsies and pathophysiologic mechanisms of the photoparoxysmal response. Neurology *53*, 926–932.

37. Takahashi, Y., Fujiwara, T., Yagi, K., and Seino, M. (1999b). Wavelength dependence of photoparoxysmal responses in photosensitive patients with epilepsy. Epilepsia *40*, 23–27.

38. Stoker, G., Drummond, K., Massengale, C., Bahr, C., Lin, S., and Vaughn, S. (2019). Dyslexia and Related Disorders Reporting Study (American Institutes for Research).

39. Stein, J. (2014). Dyslexia: the role of vision and visual attention. Curr. Dev. Disord. Rep. *1*, 267–280.

40. Singleton, C., and Trotter, S. (2005). Visual stress in adults with and without dyslexia. J. Res. Read. *28*, 365–378.

41. Ikeshita, H., Yamaguchi, S., Morioka, T., and Yamazoe, T. (2018). Effects of highlighting text on the reading ability of children with developmental dyslexia: A pilot study. Int. J. Emerg. Technol. Learn. *13*, 239.

42. Wahl, S., Engelhardt, M., Schaupp, P., Lappe, C., and Ivanov, I.V. (2019). The inner clock—blue light sets the human rhythm. J. Biophotonics *12*, e201900102.

43. Hatori, M., Gronfier, C., Van Gelder, R.N., Bernstein, P.S., Carreras, J., Panda, S., Marks, F., Sliney, D., Hunt, C.E., Hirota, T., et al. (2017). Global rise of potential health hazards caused by blue light-induced circadian disruption in modern aging societies. NPJ Aging Mech. Dis. *3*, 9.

44. Tähkämö, L., Partonen, T., and Pesonen, A.-K. (2019). Systematic review of light exposure impact on human circadian rhythm. Chronobiol. Int. *36*, 151–170.

45. Sasseville, A., Paquet, N., Sévigny, J., and Hébert, M. (2006). Blue blocker glasses impede the capacity of bright light to suppress melatonin production. J. Pineal Res. *41*, 73–78.

46. Van der Lely, S., Frey, S., Garbazza, C., Wirz-Justice, A., Jenni, O.G., Steiner, R., Wolf, S., Cajochen, C., Bromundt, V., and Schmidt, C. (2015). Blue blocker glasses as a countermeasure for alerting effects of evening light-emitting diode screen exposure in male teenagers. J. Adolesc. Health *56*, 113–119.

47. Moreddu, R., Elsherif, M., Butt, H., Vigolo, D., and Yetisen, A.K. (2019). Contact lenses for continuous corneal temperature monitoring. RSC Adv. *9*, 11433–11442.

48. Rastegar, A., Škarabot, M., Blij, B., and Rasing, T. (2001). Mechanism of liquid crystal alignment on submicron patterned surfaces. J. Appl. Phys. *89*, 960–964.

49. Bechtold, I.H., De Santo, M.P., Bonvent, J.-J., Oliveira, E.A., Barberi, R., and Rasing, T. (2003). Rubbing-induced charge domains observed by electrostatic force microscopy: effect on liquid crystal alignment. Liq. Cryst. *30*, 591–598.